CONF-9205123--5

PNL-SA--20917

DE92 015762

ADVANCED MATERIALS DEVELOPMENT FOR FOSSIL ENERGY CONVERSION APPLICATIONS

J. L. Bates
L. A. Chick
J. J. Kingsley
L. R. Pederson
W. J. Weber
G. E. Youngblood

May 1992

Presented at the
Fossil Energy Materials Conference
May 12-14, 1992
Oak Ridge, Tennessee

Work supported by
the U.S. Department of Energy
under Contract DE-AC06-76RLO 1830

Pacific Northwest Laboratory
Richland, Washington 99352

ADVANCED MATERIALS DEVELOPMENT FOR FOSSIL ENERGY CONVERSION APPLICATIONS

J. L. Bates, L. A. Chick, J. J. Kingsley,
L. R. Pederson, W. J. Weber, and G. E. Youngblood

Pacific Northwest Laboratory[1]
Richland, Washington 99352

J. K. Hurst, A. E. Bell, D. W. Grainger, S. B. Rananavare,
D. K. Roe, and D. H. Thompson

Oregon Graduate Institute
Beaverton, Oregon 97006-1999

ABSTRACT

Research activities being conducted as part of this project include: (1) fundamental studies of electrochemical processes occurring at surfaces and interfaces in fuel cells, and (2) development of novel materials synthesis and processing methodologies for fossil energy conversion applications. Complex impedance and dc polarization studies of the electrocatalytic activity at the cathode have allowed intrinsic materials properties to be separated from extrinsic properties related to morphology. Mixed conduction in cathode materials was shown to dramatically enhance electrocatalytic activity with this approach. Combustion synthesis methods were used to prepare multicomponent perovskite catalysts in the $La_{1-x}Sr_xCo_{1-y}Fe_yO_3$ system. Electronic properties of these catalysts can be altered by adjusting the composition, which affects both catalytic activity and selectivity. Inverse micelles have been utilized to prepare nanosized nickel sulfide particles, which show promise as hydrodesulfurization catalysts for liquified coal. Self-assembling organic monolayers and derivatized inorganic surfaces have been used to control nucleation and crystal morphology of inorganic phases.

INTRODUCTION

This project, conducted jointly by Pacific Northwest Laboratory and Oregon Graduate Institute, seeks to develop advanced ceramic materials for utilization in solid oxide fuel cells and other technologies related to the broad, clean, and efficient use of fossil fuels. Objectives of this project are to (1) identify and develop new, electrically conducting materials for use as electrolytes, electrodes, bipolar connections, membranes, and catalysts in solid-state electrochemical processes; (2) develop a fundamental understanding of molecular processes associated with advanced electrochemical and catalytic systems; and (3) develop novel materials synthesis and processing

[1]*Operated by Battelle Memorial Institute for the U. S. Department of Energy Under Contract DE-AC06-76RLO 1830.*

methodology to improve quality, reduce cost, and/or provide the capability to produce new materials, forms, and structures.

ELECTROCHEMICAL STUDIES

Electrocatalytic Reactions at the Cathode

To date, performance of a solid oxide fuel cell (SOFC) has been limited by slow oxygen reduction at the cathode-electrolyte interface. The electrochemical activity for an SOFC cathode is a measure of the production of an ionic electrical current due to the oxygen reduction reaction at the cathode-electrolyte interface. This activity can be quantified by measuring the relative rate of oxygen reduction. The goal for a SOFC cathode is to achieve a high and stable oxygen reduction rate, or a low and stable cathodic polarization resistance.

Oxygen reduction rates should depend on: (1) the rate at which reacting constituents arrive at the reaction sites, including the local partial pressure of oxygen, (2) the number of available reaction sites, (3) the activation energy for reaction, and (4) the operating temperature. The first of these can depend on diffusion pathways through the cathode material (cathode morphology) and is very important in SOFC design. However, in selecting optimum electrode materials, it is important to perform measurements that can eliminate the effects of cathode morphology and focus instead on intrinsic electrochemical properties of the cathode material.

The unbonded interface cell (UIC) design provides an experimental approach for accomplishing this objective. In this cell design, a small pellet of electrode material with a flat but roughened surface (ground with a 15 micron diamond wheel) is pressed against a similarly roughened electrolyte material. The rough mating surfaces make multiple point contacts. The surrounding gas atmosphere easily flows between the rough surfaces and uniformly reaches the physical boundary line surrounding the cathode/electrolyte point contacts. This boundary line is called the triple phase boundary (tpb). The length of the tpb represents the surface region along the tpb on which oxygen reduction takes place, and is referred to as the "effective reaction length" or ERL. Using impedance spectroscopy with the UIC design or by measuring the circumference of cathode contact points with the electrolyte, the ERL can be estimated.

Once the ERL is defined for a particular interface, the desired goal of removing interface morphology can be achieved. The normalized reaction rate, or "specific activity" is defined by

$$\text{Specific Activity} = (\text{ERL} \times R_p)^{-1} \quad (\text{S/cm}) \qquad (1),$$

where R_p is the polarization resistance obtained from impedance spectroscopy measurements or from the initial slope of dc polarization measurements. With units of electrical conductivity, the specific activity is an intrinsic material property, independent of morphology. When using the UIC design, ERL and R_p can generally be determined from a single impedance spectroscopy scan for a given set of operating conditions (oxygen partial pressure, temperature, applied potential).

For mating electrode-electrolyte surfaces with multiple point contacts separated by distances large in comparison to r, the net contact resistance for "i" parallel point contact resistances is given by the Newman equation[1]:

$$R_c = 1/4\ \sigma\Sigma r_i \qquad (2),$$

where σ is the conductivity of the electrolyte. The total length of tpb between surfaces with multiple point contacts is then $2\pi\Sigma r_i$. The ERL, in units of length, can then be calculated:

$$ERL = 2\pi/4\sigma R_c \qquad (3).$$

Very good agreement has been obtained between ERL values determined geometrically from an SEM or optical micrograph and those obtained from the contact resistance (from impedance measurements) following equation (3). The ERL calculated using equation (3) for a single, truncated, cone-shaped platinum bead on yttria-stabilized-zirconia in a UIC was 2.05±0.15 mm. The circumference of the truncated cone top measured from an optical micrograph was 2.16 mm, in excellent agreement. We have reproducibly determined the ERL for a variety of surface types, independent of the composition of the electrode material.

The specific cathodic activity of electrode/stabilized zirconia interfaces using the UIC design were evaluated, in which the electrode was platinum or a substituted lanthanum or yttrium manganite. These determinations were made as a function of the oxygen partial pressure and temperature, as shown in Figure 1. The activation energies for the reduction of oxygen in air varied little for quite different electrode materials. Values of 1.63, 1.90, and 1.70 eV were obtained for $Y_{0.5}Ca_{0.5}MnO_3$ (YC5M), $La_{0.9}Sr_{0.1}MnO_3$ (LS1M), and platinum, respectively. Similar results (1.85 eV) have been reported by Mizusaki, et al for $La_{0.6}Ca_{0.4}MnO_3$ on stabilized zirconia[2]. These results imply that the nature of the rate-determining step in the cathodic reduction of oxygen is similar for each electrode/electrolyte interface.

While activation energies for oxygen reduction at the cathode have exhibited little variation for different electrode/electrolyte combinations, specific activities (electrocatalytic activities divided by the magnitude of the ERL) varied by orders of magnitude. Representative results obtained at or extrapolated to 960°C for a series of La(Sr)MnO_3 (LSM) compounds, YC5M, and platinum are

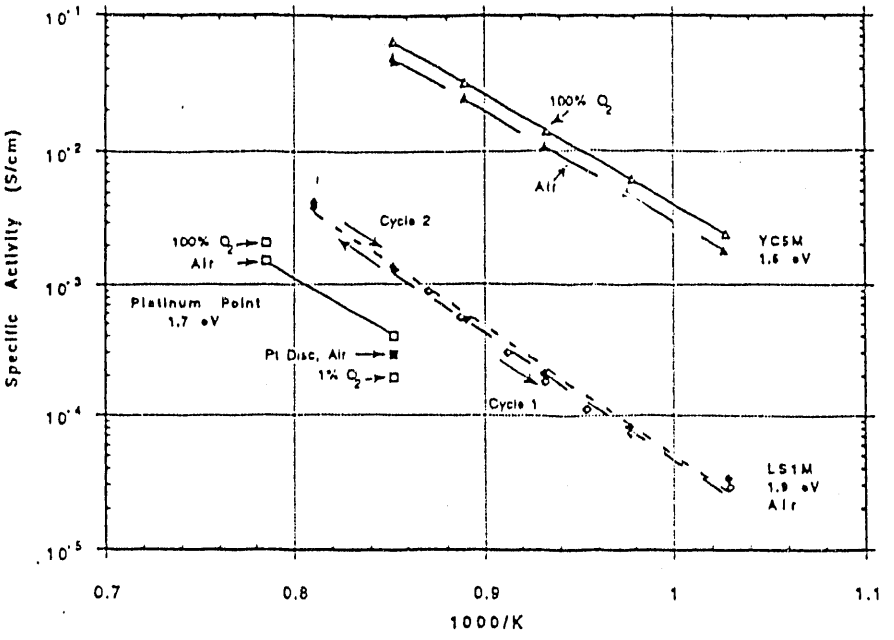

Figure 1. Temperature dependence of the specific activity of various cathode/electrolyte interfaces, measured using complex impedance spectroscopy. Specific activities are determined by dividing the electrocatalytic activity by the ERL, allowing intrinsic properties of cathode materials to be compared.

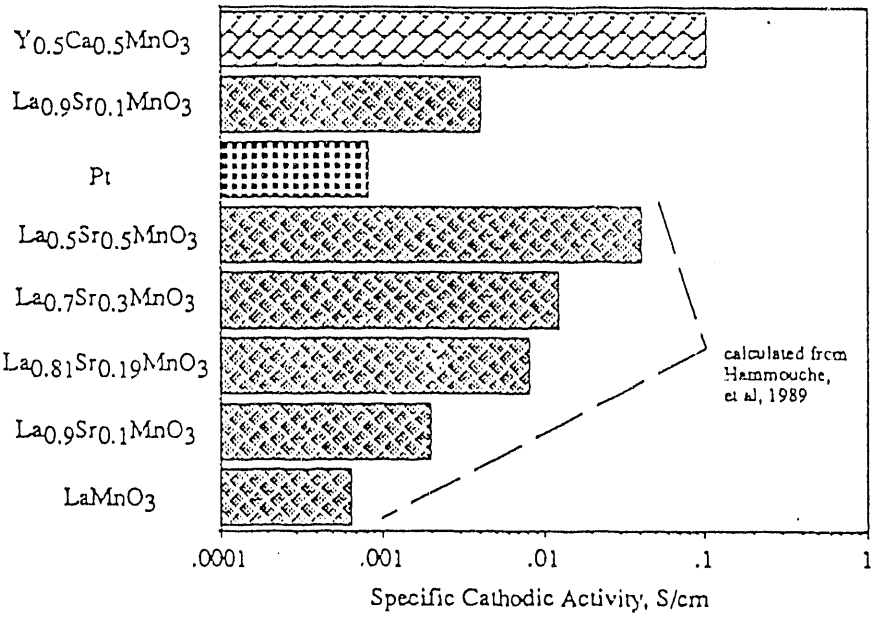

Figure 2. Specific electrocatalytic activity for oxygen reduction at the cathode/electrolyte interface for various electrode materials at 960°C. Enhanced electrocatalytic activity is attributed to an expansion of active surface sites, a result of mixed conduction in cathode materials.

given in Figure 2. Included in this figure are specific activities calculated from dc polarization curves given by Hammouche, et al[3]. Platinum resulted in among the lowest of the specific activities. For the LSM compounds, specific activities rose substantially as the extent of strontium substitution was increased. The highest electrocatalytic activity encountered to date was obtained with YC5M/zirconia interfaces.

Trends in electrocatalytic activity with electrode compositional changes are consistent with expected variations in electrode conductivity. For platinum-zirconia interfaces, oxygen reduction can only occur at the triple phase boundary and oxygen anions can migrate only within the zirconia electrolyte. While electrons can move freely in platinum, oxygen atoms or anions are immobile. Similarly, oxygen anion conduction in unsubstituted lanthanum manganite is quite low. Substitution of a divalent cation on the A-site of manganites is known to create holes via the promotion of Mn^{3+} to Mn^{4+}, thus enhancing the electrical conductivity of the material. Oxygen vacancies can also be created electrochemically, which then contribute to enhanced ionic conductivity within the electrode materials[3]. In this situation, oxygen reduction can occur not only at the triple phase boundary but on part of the electrode surface as well. The use of substituted manganites as cathodes appears to augment active surface sites for oxygen reduction, by more than two orders of magnitude in some cases.

Choice of cathode materials can be of significant importance in minimizing the overpotential in an SOFC. The following estimates are intended to illustrate this point. An acceptable fuel cell cathode might operate at 960°C with a current density J=250 mA/cm^2 in air[4]. The cathodic overpotential, which should be less than perhaps 50 mV, can be estimated from:

$$\eta_c = J\ (mA/cm^2) \times [\text{specific activity } (S/cm) \times ERL\ (cm/cm^2)]^{-1} \qquad (4).$$

The specific cathodic activity is an intrinsic property of the cathode/electrolyte interface, while the ERL is an extrinsic, materials processing property. A typical value for a thin, porous oxide cathode material sintered on a dense zirconia electrolyte is 10^3 cm/cm^2, although this value could vary considerably[2,5]. For LS1M (10 percent Sr substitution for La), the specific activity was measured at 0.004 S/cm at 960°C, leading to an estimate of the cathodic overpotential of more than 60 mV following equation (4). For YC5M (50 percent Ca substitution for yttrium), the specific activity was found to be 0.1 S/cm, leading to a cathodic overpotential estimate of 2.5 mV. Thus, both high electrocatalytic activity and effective reaction length are necessary for optimum performance of the fuel cell.

Electrocatalytic Reactions at the Anode

Electrochemical studies of reactions occurring at the anode/electrolyte interface are also being investigated. For this purpose, a reactor was designed and constructed with two compartments separated by a stabilized zirconia disk. Platinum electrodes were deposited onto both sides of the zirconia disk. Mixtures of oxygen and fuel (e. g. methane, ethane, ethylene, methanol, or carbon monoxide) are delivered to the fuel side (anode) and the potential or current through the cell externally controlled, in contrast to the normal operation of an SOFC. Vayenas and coworkers have reported large changes in catalyzed reaction rates under similar conditions, depending on the current through the zirconia electrolyte[6]. Vayenas hypothesized that this electrochemical promotion effect was related to the work function of the metal catalyst due to the increased activity of electrons at the triple-phase boundary of the zirconia electrolyte, platinum electrode, and gas reactant mixture. Because electrochemical promotion has been observed even when current flow through the electrolyte was reversed, there exists some doubt as to the role of catalyst work function on catalytic activity.

The relation of the physical state of the catalyst on activity is of current interest. Previously, thick electrode layers have been prepared by the thermal decomposition of metal paints or pastes. These thick layers were found to have very slow (minutes to hours) response times to changes in reaction conditions, especially changes in applied potential. Also, they do not have a favorable combination of the relative areas of the three phases - gas, electrolyte, and catalyst - required for efficient catalysis. Sputtered metal electrodes do provide this control, with much improved response times to changes in reaction conditions.

SYNTHESIS OF ADVANCED CATALYST MATERIALS

Combustion Synthesis of Sr-Substituted $LaCo_{0.4}Fe_{0.6}O_3$ Catalysts

Strontium-substituted $LaCo_{1-y}Fe_yO_3$ perovskites have been found to exhibit excellent mixed ionic and electronic conductivity, depending on the extent of substitution[7,8]. The materials are expected to find application in gas separation membranes by oxygen permeation, as electrodes in high temperature fuel cells, and as combustion catalysts. The key advantage offered by these

perovskite materials is the ability to tailor electronic properties by adjusting their composition, which are related to catalytic activity and selectivity.

These materials are usually prepared by conventional solid state reactions between corresponding oxides or by the decomposition of solutions containing metal nitrates and acetates. Such techniques require relatively high temperatures (>1000°C) for the formation of single phase perovskites and often yield inhomogeneous powders. Although many other wet chemical methods such as co-precipitation have been successful in producing single or two component oxides, they have inherent limitations in producing homogeneous ternary or higher multicomponent oxides.

Fine particles of $La_{1-x}Sr_xCo_{0.4}Fe_{0.6}O_3$, where x ranged from 0.0 to 0.8, were successfully prepared by combustion synthesis methods, followed by calcination of the resulting powders. Combustion reactions were performed using precursor solutions containing the corresponding metal nitrates (oxidizer) and glycine(fuel). The initiation temperature for combustion of the precursor was approximately 250°C. The combustion-derived ash consisted of very fine, mixed oxides. Following calcination at 850°C for 6 hours, these powders were converted to a single crystallographic phase. The primary particle size of the calcined product was approximately 100 nm, formed into hard agglomerates several hundred nanometers in diameter. For x=0.0-0.4, the product crystallized into an orthorhombic structure; for x=0.6-0.8, a cubic structure was obtained. Surface areas (BET) of the products ranged from 18-32 m^2/g.

The $La_{1-x}Sr_xCo_{0.4}Fe_{0.6}O_3$ powders were found to be active catalysts for the decomposition of hydrogen peroxide in alkaline solutions. Relative rates of reaction were nearly linearly dependent on the extent of strontium substitution. These reactions were conducted at 70°C using 10 mg of catalyst and 10 μL of 30% hydrogen peroxide in a stirred vessel containing 50 mL of 0.1 M NaOH. Catalytic activity for this particular reaction has been related previously to the surface concentration of oxygen vacancies.

Inverse Micelle Synthesis of Nickel Sulfide Coal Liquefaction Catalysts

Asphaltenes, derived from solvent-refined coal and heavy crude oil feed stock, contain significant (>3 percent) amounts of sulfur. We have developed a room temperature synthesis of a nickel sulfide hydrodesulfurization catalyst necessary to upgrade asphaltenes for cracking applications. The synthetic method exploits nanocompartmentalization of water and oil in surfactant-organized media (microemulsions) to fabricate ultrastable transition metal sulfides 2-4 nm in diameter.

Nickel sulfide nanoparticles were synthesized in an inverse micellar phase, with the microemulsion consisting of nonionic surfactant, hexadecane, and 1.25 percent solution of nickel chloride (46:46:8 by weight). Transmission electron microscopy (TEM) examinations revealed a diffuse micellar structure prior to the precipitation reaction. The reaction was carried out by adding a stoichiometric amount of ammonium sulfide solution. The final micellar water concentration was then adjusted to 8 percent. In Figure 3, a TEM bright field image taken immediately after the reaction shows a well-defined spheroidal structure. Initially formed amorphous nickel sulfide converted into crystalline forms over a period of two weeks.

Figure 3. Nickel sulfide nanoparticles grown in an inverse micellar phase.

Catalytic nanoparticles stabilized in microemulsions will be potentially useful in the development of efficient and easily transportable active catalysts for dehydrosulphurization and hydrogenation of liquids derived from coal, and catalysis in general. If these microemulsions are thermodynamically stable, then it opens new avenues for the studies of nucleation phenomena in restricted geometries.

Organic Thin Films as Templates for Controlled Nucleation of Inorganic Particles

Two different but closely related approaches have been taken to controlling the growth of inorganic phases: (1) nucleation and growth on derivatized inorganic microporous supports, and (2) nucleation and growth on preorganized templates using self-assembling monolayers. These efforts should illustrate key principles involved in controlling nucleation site density and crystal morphology.

Production of oriented catalyst particles on inorganic microporous supports is being pursued. In principle, these composite materials could serve as integrated catalyst membranes capable of performing both a catalytic role and a separations function while withstanding the high temperatures used in cracking, water gas shift, and other industrial processes. We have chosen to

study the crystallization of hematite (Fe_2O_3) on sebacic acid (1,10-decanedioic acid)-derivatized Anotec membranes (0.2 micron pore diameter, ca. 50 micron pore length, 47 mm membrane diameter) due to the relevance of this iron oxide in methanol oxidation, ammonia oxidation, water gas shift reaction, and desulfurization processes. This product can readily be converted to magnetite by a reductive hydrothermal treatment.

To prepare oriented iron oxide particles, alumina membranes were first coated with a tetrahydrofuran solution of sebacic acid. The membranes were air-dried and placed in a two-chamber apparatus. Aqueous solutions of ferric nitrate and nitric acid were placed in opposite chambers and the solutions allowed to diffuse together through the membrane (higher density ferric nitrate solution on top). Percolation of nitric acid through the pores resulted in forced hydrolysis of $Fe(H_2O)_6^{2+}$ at the membrane surface. Immobilized Fe(III) sites on the sebacic acid-derivatized surface served as nucleation points for crystal growth.

It was found that Fe_2O_3 particles grew on the derivatized membrane surface that faced the iron solution. A substantially smaller fraction was found as spheroidal particles and needles within the pores. Crystals grew as 0.1 micron by >4 micron needles from attachment sites at the alumina membrane surface. Pores of the membrane were found to become smaller as the particles grew.

Polymer self-assembly is the second means of controlling nucleation and growth of inorganic crystals. Ultrathin polymer films were formed by spontaneous adsorption from organic solutions. The polymers are designed with four architectural features: (1) flexible spacer groups in the backbone and side chains to facilitate organization; (2) long alkyl side chains to promote self-assembly and side-chain association; (3) anchoring groups to bind polymers to surfaces; and (4) functional groups for further surface chemistry.

Copolymerization of acrylate monomers followed by functionalization via polymer analog reactions was the route chosen. A wide variety of side chains and functional groups can be added by these methods. Film thicknesses and degrees of side-chain organization are controlled by side-chain lengths (longer chains provides better side association, and increased organization via van der Waals interactions). Anchoring groups include thiols for Au, Ag, Pt, and other metal substrates and silanes for oxide surfaces.

Film thicknesses averaged 3-5 nm (single monolayers) as measured by ellipsometry. Stability of these films has been measured under hexadecane reflux at 85°C for 28 hours. While monomeric analogs of these films were removed after 6 hours of this treatment, polymer films remained fully intact for the duration of the reflux. This attests to the increased film adhesion resulting from the use of many anchoring side chains (multipoint attachment).

Addition of a third monomer containing functional groups (amines, thiols, and carboxylic acids) into the polymer backbone provides accessible functionalities to immobilize catalysts on surfaces in high densities. Moreover, use of chelating groups (carboxylic acids, sulfonates,

phosphates) in the backbone allows construction of nucleation sites for inorganic phases. We are currently concentrating on nucleating the photoactive CdS and ferromagnetic species (Fe and Mn compounds) in high density and controlled crystalline structure on these assembled interfacial templates.

ACKNOWLEDGEMENTS

The authors appreciate assistance from G. W. Coffey, G. D. Maupin, D. E. McCready, and R. W. Stephens.

REFERENCES

1. J. Newman, "Resistance for Flow of Current to a Disk", *J. Electrochem. Soc.*, p. 501-502, 1966.

2. J. Mizusaki, H. Tagawa, K. Tsuneyoshi, and A. Sowata, "Reaction Kinetics and Microstructure of the Solid Oxide Fuel Cell's Air Electrode $La_{0.6}Ca_{0.4}MnO_3$/YSZ", *J. Electrochem. Soc.* 138(7), p. 1867-1873, 1991.

3. A. Hammouche, E. Siebert, and A. Hammou, "Crystallographic, Thermal, and Electrochemical Properties of the System $La_{1-x}Sr_xMnO_3$ for High Temperature Solid Electrolyte Fuel Cells", *Mat. Res. Bull.* 24, p. 367-380, 1990.

4. S. C. Singhal, "Solid Oxide Fuel Cell Development at Westinghouse", in *Proceedings of the 2nd International Symposium on Solid Oxide Fuel Cells*, eds. F. Grosz, B. Zeger, S. C. Singhal, and O. Yamamoto, p. 25-33, 1991.

5. L. G. J. de Hart, K. J. de Vries, A. P. M. Carvalho, J. R. Frade, and F. M. B. Marques, "Evaluation of Porous Ceramic Cathode Layers for Solid Oxide Fuel Cells", *Mat. Res. Bull.* 26, p. 507-517, 1991.

6. C. G. Vayenas, , S. Bebelis, and S. Ladas, "Dependence of Catalytic Rates on Catalyst Work Function", *Nature* 343, p. 625-627, 1990.

7. Y. Teraoka, T. Nobunaga, K. Okamoto, N. Miura, and N. Yamazoe, "Influence of Constituent Metal Cations in Substituted $LaCoO_3$ on Mixed Conductivity and Oxygen Permeability", *Solid State Ionics* 48, p. 207-212, 1991.

8. Y. Teraoka, H. M. Zhang, K. Okamoto, and N. Yamazoe, "Mixed Ionic-Electronic Conductivity of $La_{1-x}Sr_xCo_{1-y}Fe_yO_{3-\delta}$ Perovskite-Type Oxides", Mat. Res. Bull. 23, p. 51-58, 1988.

DATE
FILMED
8/12/92